ISSN 1547-4771, Physics of Particles and Nuclei Letters, 2019, Vol. 16, No. 6, pp. 835–841. © Pleiades Publishing, Ltd., 2019.

METHODS
OF PHYSICAL EXPERIMENT

Validation and Correction for ^{208}Tl Activity to Assay ^{232}Th in Equilibrium with Its Daughters

Omar Abo-Bakr Omar[a], *, Mohamed A. E. Abdel-Rahman[a], and Sayed A. El-Mongy[b]

[a] *Nuclear Engineering Department, Military Technical College, Kobry El-kobbah, Cairo, Egypt*

[b] *Nuclear and Radiological Regularity Authority of Egypt (ENRRA), Cairo, Egypt*

**e-mail: omar805805805@gmail.com*

Received June 15, 2019; revised July 16, 2019; accepted July 18, 2019

Abstract—The natural radioactivity measurements and analysis of ^{232}Th have been studied using γ-ray spectroscopy depending on its decay daughters in equilibrium; ^{208}Tl of 583.19 keV, ^{228}Ac of (911.2 and 968.97 keV) and ^{212}Pb of 238.63 keV. When using these gamma transitions to calculate the ^{232}Th specific activity, the ^{208}Tl daughter of 583.19 keV gamma line with its 0.845 branching ratio gives activity of approximately 33.94% less than the other gamma transitions. This article is trying to explain and validate this difference and discrepancy that may encounter analysts during calculation of ^{232}Th activity based on ^{208}Tl (583.19 keV) gamma line. Very efficient HpGe detector was used to carry out this work. The MDA and figure of merit as functions of HpGe and energy sensitivity were calculated and tabulated. This issue was verified and validated using Black sand and natural environmental samples. A correction factor was proposed and applied on the 583 keV line of these samples that contain ^{232}Th in equilibrium with its daughters to minimize and eliminate the abovementioned difference in the calculated ^{232}Th specific activity.

Keywords: ^{232}Th series, validation of ^{208}Tl γ-line correction, black sand, natural samples

DOI: 10.1134/S1547477119060505

1. INTRODUCTION

In general, accurate determination of thorium in ores is an objective of states planning to use thorium either for R&D or fuel of research and nuclear power plants. It can be identified and amounted by destructive and non-destructive assay techniques. NORMs mean naturally occurring radioactive materials and it is found in nature since the earth creation. NORMs were formed in supernovae and the primary particles from our universe continually bombard the forming earth's crust. The NORMs can be found almost everywhere, in soil, air, water supplies and oil. Therefore, NORMs always has been a part of our world and hence the sources of radioactive isotopes in the environment that can be divided into two main categories, natural sources that contribute by 96% of total radiation dose to the world population and on the other hand artificial sources contribute by 4% of total radiation dose to the world population [1, 2].

The terrestrial (primordial) radionuclides are main source of (NORMs) in the environment. In addition, there are also three naturally decay series; ^{238}U, ^{232}Th and ^{235}U [3].

2. EXPERIMENTAL WORK

Most of gamma-ray spectroscopic studies for analysis of ^{232}Th decay series use its gamma decays daughters such as ^{208}Tl (583.19 keV), ^{228}Ac (911.2 and 968.97 keV) and ^{212}Pb (238.63 keV). This is due to the fact that these gamma lines have the highest branching ratio and have approximately no energy interferences with the other daughter's transitions [4–6].

2.1. Measurements Arrangement and Detection System Set-Up

In this study, the collected samples analyzed using a high-purity germanium (HpGe) [7] with relative efficiency ~50%. The main specifications of the detection system are given in Table 1. The HpGe detector with its built-in preamplifier is operated at high voltage power ~3 kV. For cooling the Ge crystal, it was in contact with cold finger which is fully immersed in liquid nitrogen (LN_2) at (–77°C) thermally isolated under vacuum in cryostat to reduce the noise of leakage current. The output signal was connected to spectroscopy shaping amplifier followed by a multi-channel analyzer (MCA) with (16 384) channels. To avoid contribution of the background radia-

Table 1. The main specifications of the HpGe detector [7]

Detector model:	GC5019
Preamplifier model:	2002CSL
Cryostat model:	7500SL
Relative efficiency:	≥50%
Resolution:	≤1.9 keV@1.33 MeV
Peak/Compton (P/C):	≥ 64:1

tion and various natural radiation sources in nearby surrounding to the measured activity of samples, a lead shield with approximately 10 cm thick with an inner layer of 1 mm tin and 1.6 mm copper to minimize the participation from Pb X-ray florescence and to inhibit the effect of x-rays peaks were used [3, 8, 9].

2.1.1. Calculation of detector resolution. HPGe resolution is the main specific characteristic than other solid-state detectors and it can be determined by different parameters like conversion factor and full width at half maximum (FWHM) and full width at tenth maximum (FWTM). It has been achieved using ^{60}Co radioisotope, which was counted for 30 min to obtain high enough number of counts for its two energy peaks; 1173.2 and 1332.5 keV. The conversion factor was calculated using Eq. (1).

$$\text{Conversion factor} = \frac{\Delta E}{\Delta N}, \quad (1)$$

where ΔE is the difference between two energy peaks in keV (1332.5–1173.2 = 159.3 keV).

ΔN is the number of channels between the two peaks. The conversion factor should be in the range of (0.16 keV/channel). If it isn't then something is set up improperly [7]. The calculated conversion factor was found to be 0.157 which is in the proper range.

2.1.2. Peak/Compton (P/C) ratio calculation. The peak to Compton ratio (P/C) of coaxial detectors depends on many characteristics like resolution, efficiency, as well as peak shape, charge collection. The peak to Compton measurement has been done under the same condition as the resolution measurement was done but it uses peak height not peak area in calculating the (P/C) value, the Compton region that has been used for (P/C) calculations as defined in IEEE standard 325, is from 1040 to 1096 keV for ^{60}Co [7, 10] Finally, the (P/C) ratio was calculated using Eq. (2).

$$(\text{P/C}) = \frac{\text{number of counts in the highest channel of 1332.5 keV peak}}{\text{average counts per channel (1040 keV and 1096 keV)}}. \quad (2)$$

The (P/C) ratio result was found to be (74.7 : 1) which is matched and better than the certified value as shown in Table 1.

2.1.3. Relative efficiency calculation. Relative efficiency calculation was performed using point standard source ^{60}Co which placed 25 cm away from the end-cap and counted for 1000 s [7]. It was calculated using Eq. (3).

$$\text{Relative efficiency (\%)} = (\text{N/T}) \times (1/R_s) \times (1/1.2\times10^{-3}) \times 100, \quad (3)$$

where N, is the number of counts in 1332.5 keV peak. T is the preset time. R_s, is the source strength in gamma rays per second. The 1.2×10^{-3} is the efficiency of 3" × 3" NaI detector at 25 cm. The relative efficiency result was found to be 51.6 which is almost as the certified value given in Table 1.

2.2. Energy Calibration

Energy calibration of the HpGe detector system were performed using IAEA certified reference material RGU-1 [11] which has been counted for 24 h to obtain high enough statistics. A plot between the channel number and the energy was obtained as shown in Fig. 1 with its correlation Eq. 4 [12].

$$\text{Energy (keV)} = 0.167 + 0.1747 \times \text{channel number}. \quad (4)$$

2.3. Efficiency Calibration

The absolute photo-peak efficiency which depends on many parameters like; source and detector geometry–gamma energy–density–distance between the source and detector–specifications of the used HPGe detector, was measured. The efficiency calibration of the detector carried out using certified reference material IAEA (RGU-1) [11], which counted three times for 86 400 s and then Microsoft excel program used to calculate the efficiency curve at every gamma energy using Eq. (5). Then, the Genie 2000 program was used to obtain the correlation as shown in Fig. 2 [3, 13].

$$\xi_{abs} = \frac{c}{I_{\gamma(E)} t A_c m}, \quad (5)$$

where ξ_{abs}, is the detector photo-peak efficiency at specific energy and conditions. C, is the number of counts at certain region of interest in the spectrum minus the number of counts in background spectrum at the same region of interest. $I_{\gamma(E)}$, the emission probability of gamma having certain energy per disintegration. t, the counting time 24 h (86 400 s). A_c is the activity concentration of the reference source (Bq/kg). m, mass of the reference source in (kg).

The results of efficiency calculations for different gamma energies for ^{232}Th activity using Eq. (5) are given in Table 2.

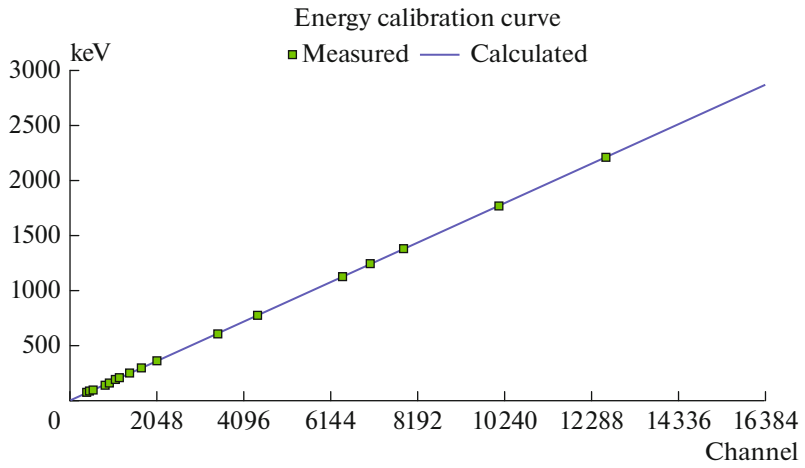

Fig. 1. Energy calibration curve of HpGe spectrometer.

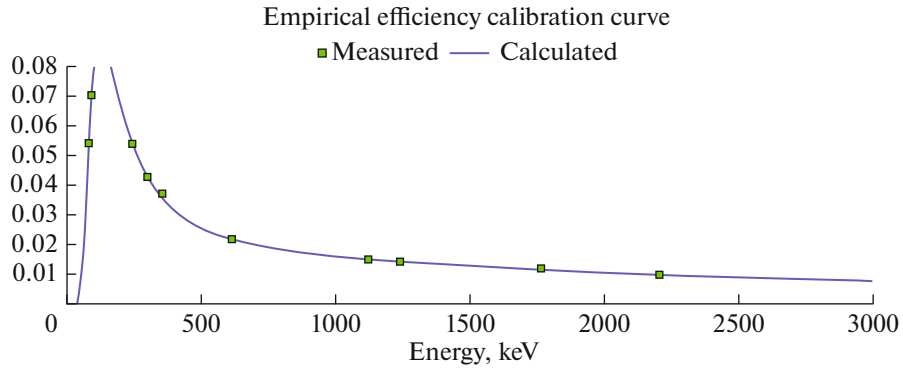

Fig. 2. Efficiency calibration curve for (RGU-1) using Genie2000.

2.4. Samples Collection and Preparation

Evaluation of the terrestrial radioactivity levels (mainly ^{232}Th through its decay daughters) and its radiological hazard indices in black sand samples of Rashid area and other natural environmental area are topic of this work. Many natural soil samples were collected then prepared through the following steps [3]. Sieving step: the collected samples sieved using a 2 mm mesh to obtain a uniform particle size and also because no radioactive materials exist on large size sand surface [14]. Drying step: The sieved samples

Table 2. The system efficiency calculation results

Parent	Radionuclide (daughter)	Energy, keV	Efficiency, ξ	Branching ratio ($I\gamma E$), %
^{238}U	^{214}Pb	295.4	0.043405	18.5
^{238}U	^{214}Pb	351.92	0.035794	35.8
^{238}U	^{214}Bi	609.31	0.021674	44.8
^{238}U	^{214}Bi	1120.28	0.015148	14.8
^{232}Th	^{212}Pb	238.63	0.055161	43.6
^{232}Th	**^{208}Tl**	**583.19**	**0.022401**	**84.5**
^{232}Th	^{228}Ac	911.2	0.016841	26.6
^{232}Th	^{228}Ac	968.97	0.016303	16.2
^{40}K	^{40}K	1460.83	0.013241	10.88

Table 3. The calculated MDA and Figure of merit (FOM) of the detection system

Parent	Radionuclide (daughter)	γ energy line, keV	Efficiency ξabs	Branching ratio *I*γ, %	Average *B.G.C*	*FOM* ($\times 10^{-1}$)	*MDA*, Bq/Kg
^{232}Th	^{212}Pb	238.63	0.055161	43.6	1633	1.609	0.3 ± 0.003
^{232}Th	**^{208}Tl**	**583.19**	**0.022401**	**84.5**	**620**	**0.699**	**0.24 ± 0.001**
^{232}Th	^{228}Ac	911.2	0.016841	26.6	451	0.543	0.85 ± 0.04
^{232}Th	^{228}Ac	968.97	0.016303	16.2	267	0.860	1.11 ± 0.03
^{238}U	^{214}Pb	295.4	0.043405	18.5	1057	1.539	0.73 ± 0.03
^{238}U	^{214}Pb	351.92	0.035794	35.8	1020	1.085	0.45 ± 0.02
^{238}U	^{214}Bi	609.31	0.021674	44.8	1102	0.368	0.61 ± 0.02
^{238}U	^{214}Bi	1120.28	0.015148	14.8	397	0.499	1.6 ± 0.08
^{40}K	^{40}K	1460.83	0.013241	10.88	1240	0.122	4.4 ± 0.06

were dried in a drying oven at 110°C until removal of the moisture because the existence of moisture may affect the samples analysis results as it may act as attenuation material [15].

The prepared samples were then weighted and transferred to the Marinelli containers and sealed to kept undisturbed for 28 days to attain material equilibrium between ^{232}Th and its decay chain daughters [13].

3. RESULTS AND DISCUSSION

3.1. Minimum Detectable Activity (MDA) and Figure of Merit (FOM) Calculations

When detecting environmental radioactivity, it is necessary to determine the MDA of the counting system, environmental background radiation in the detection system can differ from place to another one and come from different sources like (10% of the background created through the detector itself—40% from its environment—10% from radon in the air—40% due to interactions of cosmic rays with the detector and its shield) [13].

The MDA calculations were carried out using Eq. (6) [3, 13] and the obtained results are given in Table 3.

$$MDA = \frac{4.66\sqrt{B.G.C}}{I_{\gamma(E)} t \xi_{abs} m}, \quad (6)$$

where *MDA* is the minimum detectable activity of certain energy (Bq/kg). ξ_{abs}, is the detector photo peak efficiency at certain energy and known measurement condition. *B.G.C* is the number of counts at certain region of interest in the back ground spectrum. *m* is the mass and assuming an average mass of all samples and equal to 0.3 kg.

Figure of merit (FOM) calculations were assessed using Eq. (7) [16] and the obtained results are given in Table 3. Figure of merit (FOM) parameter can be used to characterize the performance of two or more detection systems and also can be used to determine the gamma lines that can be used to measure the activity of ^{232}Th with the highest precision [16]. Figure of merit calculations results obtained are given in Table 3.

$$FOM = \frac{(\xi_{abs})^2}{B.G.C}, \quad (7)$$

where *B.G.C* is the count rate at certain region of interest in the background spectrum. ξ_{abs}, is the detector photo peak efficiency at certain energy and known measurement condition.

3.2. Specific Activity of ^{232}Th of Rashid Black Sand Samples

Ten representative black sand samples (Ac-1–Ac-10) were investigated for assay of ^{232}Th. These samples were collected from ten different locations along the Rashid city coast, the activity, in Bq kg^{-1}, of gamma lines emitted from daughter nuclides of ^{232}Th decay series in the measured samples were calculated. The activity concentration of **^{232}Th** in the ten samples was estimated using all the measured γ ray transitions related to their decay products, such as ^{212}Pb, ^{228}Ac and ^{208}Tl. The daughter nuclides are assumed to be in material equilibrium with their parents. Table 4 shows the activity (A_C) values for the ten black-sand samples based on the daughter nuclides of the ^{232}Th decay series including the 583 keV line of ^{208}Tl [13].

The activity of ^{232}Th decay series of these samples were varied from 94.24 to 579.84 with average value 140.38 ± 21.7 Bq/kg. The activity of ^{232}Th in samples are compared with the worldwide mean range as reported by the UNSCEAR 2000 [17]. The high activity of ^{232}Th, may be attributed to either the mobility or fixation of ^{232}Th in the crystal structure of black sand and its geochemical nature [13, 18–21].

Table 4. The activity (Bq/kg) for ^{232}Th daughters in black sand samples

Radio-isotopes	Energy, keV	Ac-BS1	Ac-BS2	Ac-BS3	Ac-BS4	Ac-BS5	Ac-BS6	Ac-BS7	Ac-BS8	Ac-BS9	Ac-BS10
Pb-212	238.63	564.90	95.34	95.20	118.94	134.26	104.78	153.62	134.92	139.92	165.69
Ac-228	338.4	533.93	83.15	129.78	152.43	150.52	129.78	128.66	134.25	129.06	137.34
Ac-228	911.07	595.16	101.55	104.65	159.44	166.75	124.57	186.77	164.31	172.66	202.06
Ac-228	968.9	626.93	99.25	111.25	132.87	140.85	118.05	159.87	143.53	147.26	171.47
Tl-208	510.7	673.98	109.07	77.66	133.21	130.66	93.68	120.50	124.69	120.75	127.35
Tl-208	**583.1**	**474.36**	**86.78**	**97.76**	**137.26**	**146.14**	**119.07**	**180.61**	**153.33**	**162.43**	**198.44**
Tl-208	2614.4	589.62	84.57	106.31	147.95	162.04	110.57	175.61	155.42	149.25	185.02

It can be observed from Table 4 that the results of ^{208}Tl gamma line (583.1 keV) are slightly different and relatively less than these calculated by the other gamma lines. This will be discussed in the next paragraph under ^{208}Tl activity correction factor.

3.3. Activity Calculations of Natural Environmental Samples Using ^{232}Th Daughters

Specific radionuclides in this decay chain are noteworthy because of their decay characteristics (^{224}Ra decays by alpha to ^{220}Rn; ^{212}Bi and ^{208}Tl are gamma emitters). The ^{232}Th activity was estimated using the γ-rays of its main decay daughters ^{208}Tl (583.19 keV), ^{228}Ac (911.2 and 968.97 keV) and ^{212}Pb (238.63 keV). A Microsoft excel program was used to calculate the average activity of ^{232}Th radionuclide assuming that material equilibrium is attained. The results of calculations for ten natural soil samples (coded from D1–D10) are given in Fig. 3, and for another ten soil samples (coded from D11–D20) as in Fig. 4.

Where the avg Ac, is the average ^{232}Th activity results using only three gamma lines of its daughters; 911.2 and 968.97 keV of ^{228}Ac and 238.63 keV of ^{212}Pb. While, Tl208 Ac is the ^{232}Th activity results based on 583.19 keV γ-line of ^{208}Tl. The Tl208Ac/avgAc is the ratio between ^{232}Th activity results when using only ^{208}Tl (583.19 keV) γ-line. When using three gamma lines of its daughters; ^{228}Ac of 911.2 keV and 968.97 keV and ^{212}Pb of 238.63 keV. EFF. is the efficiency calculations results of the detection system. B.R. is the branching ratio values of specific gamma lines.

As shown in Figs. 3 and 4, there is a difference between the calculation results of ^{232}Th activity using ^{208}Tl (583.19 keV) and the other daughters ^{228}Ac (911.2 and 968.97 keV) and ^{212}Pb (238.63 keV). In spite of, almost identical results due to the material equilibrium between ^{232}Th and its daughters must be obtained. The difference in the results can be explained based on the fact that decay chain of ^{232}Th at ^{212}Bi daughter (Fig. 5) has two probabilities of decay to reach the stable ^{208}Pb. The first one is the decay route of ^{212}Bi to ^{208}Tl through an alpha emission with probability of 35.93%. The second decay is to ^{212}Po through beta process with 64.07% probability. In other words, only 35.93% of ^{212}Bi decays to ^{208}Tl daughter, while, 100% of ^{228}Ac and ^{212}Pb decay in real material equilibrium with the parent ^{232}Th.

So, the ^{208}Tl activity value should be divided by the branching ratio (0.3594) to represent ^{232}Th equivalent [16, 22–25]. This correction for ^{208}Tl in calculation of ^{232}Th activity was also observed and given in other work [13].

Radionuclide	EEF	B. R	Energy	D1	D2	D3	D4	D5	D6	D7	D8	D9	D10
Tl-200	0.022401	0.845	583.19	7.12	4.08	2.58	3.35	5.03	3.55	2.58	5.54	4.29	4.50
Ac-228	0.0168407	0.266	911.2	22.56	12.79	7.79	8.91	16.67	10.69	8.36	18.63	13.25	12.90
Ac-228	0.0163029	0.162	968.97	24.21	13.09	8.14	9.13	16.05	11.73	7.93	17.47	13.76	14.08
Pb-212	0.0551606	0.436	238.63	17.44	10.31	6.86	7.10	12.51	9.13	7.49	14.02	10.48	10.09
			avg Ac	21.40	12.06	7.59	8.38	15.08	10.52	7.93	16.71	12.50	12.36
			Tl208Ac	7.12	4.08	2.58	3.35	5.03	3.55	2.58	5.54	4.29	4.50
			Tl208Ac/avAc	0.33	0.34	0.34	0.40	0.33	0.34	0.33	0.33	0.34	0.36

Fig. 3. The activity (Bq/kg) of ^{232}Th daughters in ten soil samples (D1–D10).

Radionuclide	EEF	B. R	Energy	D11	D12	D13	D14	D15	D16	D17	D18	D19	D20
Tl-200	0.022401	0.845	583.19	3.2	2.63	7.88	6.00	9.40	5.25	4.58	3.86	3.47	2.67
Ac-228	0.0168407	0.266	911.2	10.04	9.02	24.31	19.09	29.87	16.32	16.02	12.56	11.04	8.76
Ac-228	0.0163029	0.162	968.97	10.56	9.57	24.51	18.62	30.98	17.82	14.71	11.92	11.45	8.43
Pb-212	0.0551606	0.436	238.63	8.09	6.86	19.27	15.20	22.19	12.91	12.18	9.99	9.30	7.18
			avg Ac	9.56	8.48	22.70	17.64	27.68	15.68	14.30	11.49	10.60	8.12
			Tl208Ac	3.2	2.63	7.88	6.00	9.40	5.25	4.58	3.86	3.47	2.67
			Tl208Ac/avAc	0.33	0.31	0.35	0.34	0.34	0.34	0.32	0.34	0.33	0.33

Fig. 4. The activity (Bq/kg) of ^{232}Th daughters in ten soil samples (D11–D20).

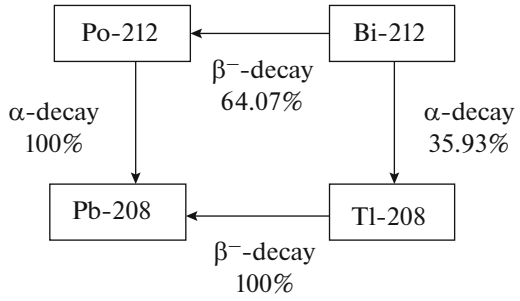

Fig. 5. The ^{212}Bi–^{208}Tl decay probability.

As shown from the results given in Figs. 3 and 4, the Microsoft excel program was used to validate that only 35.93% of ^{212}Bi decay leads to ^{208}Tl daughter. This is clear by comparison of the results of the average activity of ^{232}Th (avgAc) using only the three γ-lines 911.2, 968.97 keV and ^{212}Pb of 238.63 keV with ^{232}Th activity (Tl208Ac). When using ^{208}Tl (583.19 keV) which is presented by (Tl208Ac/avgAc), its value was found to be different from the 35.93%. Finally, the ratio (Tl208Ac/avgAc) was calculated for 20 soil samples as shown in Figs. 3 and 4. The total average of results was found to be (0.3394 ± 0.0167). In other words, a difference of about 0.3593 was found at assessment of ^{232}Th through its ^{208}Tl of 583 keV.

The difference between activity of ^{232}Th as calculated by ^{208}Tl daughter and its other daughters was also found in other published work [26].

4. CONCLUSIONS

Based on the results obtained in this study using HpGe spectrometer, the specific activity calculation of ^{232}Th based on its daughter ^{208}Tl of 583.19 keV shows different values rather than the other ^{228}Ac (911.2 and 968.97 keV) and ^{212}Pb 238.63 keV daughters. A correction factor was deduced and should be applied when using ^{208}Tl (583.19 keV) with its branching ratio 0.85 for calculation of ^{232}Th activity. This correction factor is quantified to be 0.3394 ± 0.0167**.** The difference is mainly due to the **33.9%** of ^{212}Bi decay probability that leads to ^{208}Tl daughter. The same correction is to be applied for other gamma lines of ^{208}Tl. It was applied on samples collected from Rashid black sand and natural environmental soil.

In general, accurate determination of thorium activity, by destructive or non-destructive technique, is very crucial measure to evaluate its feasibility to be used in nuclear fuel cycle.

REFERENCES

1. R. Mehra, R. G. Sonkawade, S. Kansal, and S. Singh, "Analysis of terrestrial natural radionuclides in soil samples and assessment of average effective dose," Indian J. Pure Appl. Phys. **48**, 805–808 (2010).
2. F. Ward Whicker, M. Eisenbud, and Th. Gesell, "Environmental radioactivity from natural, industrial, and military sources," Rad. Res. **148**, 402–403 (1997).
3. O. Abo Bakr, M. Abdel-Rahman, and S. A. El-Mongy, "Analysis of naturally occurring radioactive materials in environmental samples using gamma spectrometry," in *Proceedings of the 9th International Conference on Chemical and Environmental Engineering (ICEE9), 3–5 April, 2018,* MTC.
4. N. Naskar, S. Lahiri, P. Chaudhuri, and A. Srivastava, "Measurement of naturally occurring radioactive materials, ^{238}U and ^{232}Th. Part 3: Is efficiency calibration necessary for quantitative measurement of ultra-low level NORM?," J. Radioanal. Nucl. Chem. **314**, 507–511 (2017).
5. K. M. Azmary, J. Ferdous, and M. M. Haque, "Natural radioactivity measurement and assessment of radiological hazards in some building materials used in Bangladesh," Sci. Res. **09**, 1034–1048 (2018).
6. S. Yasmin, B. S. Barua, M. Uddin Khandaker, M. Kamal, M. Abdur Rashid, S. F. Abdul Sani, H. Ahmed, B. Nikouravan, and D. A. Bradley, "The presence of radioactive materials in soil, sand and sediment samples of Potenga sea beach area, Chittagong, Bangladesh: Geological characteristics and environmental implication," Results Phys. **8**, 1268–1274 (2018).

7. CANBERRA Germanium Detectors, in *GC5019* (Canberra, U.S.A., 2003), p. 91.
8. A. M. El-Arabi, "^{226}Ra, ^{232}Th and 40K concentrations in igneous rocks from eastern desert, Egypt and its radiological implications," Radiat. Meas. **42**, 94–100 (2007).
9. M. A. E. Abdel-Rahman, H. Abu Shady, and S. A. El-Mongy, "Analysis of ores and its purified constituents by γ-spectrometry with calculation of uranium isotopic atom, mass, and activity ratios," Zeitschr. Anorg. Allgem. Chem. **644**, 477–482 (2018).
10. M. W. Yii, "Determination performance of gamma spectrometry co-axial HPGE detector in radiochemistry and environment group," Nucl. Malaysia (2014).
11. IAE Agency, *Preparation and Certification of IAEA Gamma Spectrometry Reference Materials, RGU-1, RGTh-1 and RGK-1* (Int. Atomic Energy Agency, 1987).
12. M. Oddone, L. Giordani, F. Giacobbo, M. Mariani, and S. Morandi, "Practical considerations regarding high resolution gamma-spectrometry measurements of naturally occurring radioactive samples," J. Radioanal. Nucl. Chem. **277**, 579–585 (2008).
13. M. A. E. Abdel-Rahman and S. A. El-Mongy, "Analysis of radioactivity levels and hazard assessment of black sand samples from Rashid area," Egypt. Nucl. Eng. Technol. **49**, 1752–1757 (2017).
14. I. Vukašinović, D. Todorović, Lj. Životić, L. Kaluđerović, and A. Đorđević, "An analysis of naturally occurring radionuclides and ^{137}Cs in the soils of urban areas using gamma-ray spectrometry," Int. J. Environ. Sci. Technol. **15**, 1049–1060 (2018).
15. E. Gören, Ş. Turhan, A. Kurnaz, A. M. K. Garad, C. Duran, F. Uğur, and Z. Yegingil, Environmental evaluation of natural radioactivity in soil near a lignite-burning power plant in Turkey," Appl. Radiat. Isot. **129**, 13 (2017).
16. M. Dlugosz-Lisiecka, "Comparison of two spectrometric counting modes for fast analysis of selected radionuclides activity," J. Radioanal. Nucl. Chem. **309**, 941–945 (2016).
17. C. Monty, "UNSCEAR Report 2000: United Nations Scientific Committee on the effects of atomic radiation, sources and effects of ionizing radiation," J. Radiol. Protect. **21**, 83 (2001).
18. M. R. Khattab, H. Tuovinen, J. Lehto, I. E. El Assay, M. G. El Feky, and M. A. Abd El-Rahman, "Determination of uranium in Egyptian graniteic ore by gamma, alpha, and mass spectrometry," Instrum. Sci. Technol. **45**, 338–348 (2017).
19. S. F. Hassan, M. A. M. Mahmoud, and M. A. E. Abd El-Rahman, "Effect of radioactive minerals potentiality and primordial nuclei distribution on radiation exposure levels within muscovite granite, Wadi Nugrus, Southeastern Desert, Egypt," J. Geosci. Environ. Protect. **4** (3), 62–78 (2016).
20. D. Malain, P. H. Regan, D. A. Bradley, M. Matthews, T. Santawamaitre, and H. A. Al-Sulaiti, "Measurements of NORM in beach sand samples along the Andaman coast of Thailand after the 2004 tsunami," Nucl. Instrum. Methods Phys. Res., Sect. A **619**, 441–445 (2010).
21. A. Monier, S. A. E. Abdelhameid, and H. K. Fouad, "Developed method for thorium analysis in Egyptian black sand monazite fraction," Arab. J. Nucl. Sci. Appl. **39** (2006).
22. R. B. Oberer, L. G. Chiang, M. J. Norris, C. A. Gunn, and B. C. Adaline, *The Use of TI-208 Gamma Rays for Safeguards, Nondestructive-Assay (NDA) Measurements, Oak Ridge Y-12 Plant (Y-12)* (Oak Ridge, TN, 2009), p. Medium: ED.
23. M. Pope, *Identification of Naturally Occurring Radioactive Material in Sand, NSF/REU Program* (Phys. Dep., Univ. Notre Dame, 2012).
24. G. R. Gilmore, *Practical Gamma-ray Spectroscopy,* 2nd ed. (Wiley, Chichester, 2008).
25. W. F. Mueller, G. Ilie, H. Lange, M. Rotty, and W. R. Russ, "In-situ measurements and analysis of naturally occurring radioactive materials," in *Proceedings of the 3rd International Conference on Advancements in Nuclear Instrumentation, Measurement Methods and their Applications (ANIMMA), 2013.*
26. A. L. Nichols, *208Tl-Comments on Evaluation of Decay Data* (Univ. of Surrey, 2010), p. 15.